

RESEARCH

Open Access



The performance of Cu^{2+} as dissolved cathodic electron-shuttle mediator for Cr^{6+} reduction in the microbial fuel cell

Praveena Gangadharan^{1*}  and Indumathi M. Nambi²

Abstract

The study investigates the performance of Cu^{2+} as dissolved cathodic electron-shuttle mediator (dcESM) for simultaneous Cr^{6+} reduction and electricity generation in a microbial fuel cell (MFC) at pH 2 and 4 conditions. The dcESM behavior of Cu^{2+} on carbon cloth (CC) catalyzes the reduction of Cr^{6+} into Cr^{3+} at pH 2 by undergoing redox reactions. However, at pH 4, a simultaneous reduction of Cu^{2+} and Cr^{6+} was observed. Cyclic voltammetry studies were performed at pH 2 and 4 to probe the dcESM behavior of Cu^{2+} for Cr^{6+} reduction on CC electrode. Also, at pH 2, increasing the concentration of Cu^{2+} from 50 to 500 mg L^{-1} favors the Cr^{6+} reduction by reducing the reaction time from 108 to 48 h and improving the current production from 3.9 to 6.2 mA m^{-2} , respectively. Nevertheless, at pH 4, the efficacy of Cr^{6+} reduction and electricity generation from MFC is decreased from 63 to 18% and 4.4 to 1.1 mA m^{-2} , respectively, by increasing the Cu^{2+} concentration from 50 to 500 mg L^{-1} . Furthermore, the performance of dcESM behavior of Cu^{2+} was explored on carbon felt (CF) and platinum (Pt) electrodes, and compare the results with CC. In MFC, at pH 2, with an initial concentration of 100 mg L^{-1} , the reduction of Cr^{6+} in 60 h is 9.6 mg L^{-1} for CC, 0.2 mg L^{-1} for CF, and 51.3 mg L^{-1} for Pt cathodes. The reduction of Cr^{6+} (initial concentration of 100 mg L^{-1}) at pH 4 in 120 h is 44.7 mg L^{-1} for CC, 32.1 mg L^{-1} for CF, and 70.9 mg L^{-1} for Pt cathodes. Maximum power densities of 1659, 1509, and 1284 mW m^{-2} were achieved when CF, CC, and Pt, respectively were employed as cathodes in the MFC.

Keywords: Microbial fuel cell (MFC), Heavy metal removal, Hexavalent chromium, Copper, Wastewater treatment, Bioelectricity generation

Introduction

In recent years, hexavalent chromium (Cr^{6+}) is exceedingly prevalent in various industrial effluents, and is often discharged from metallurgy, electroplating, leather tanning, and textile industries [1]. Cr^{6+} is a well-known mutagen, teratogen, and carcinogen [2]. The discharge of Cr^{6+} to the environment is of critical concern because: (i) of its non-biodegradable nature; (ii) it undergoes various transformations and forms toxic, carcinogenic compounds; and (iii) it is bioaccumulative [3]. The existing traditional

treatment techniques for the removal of Cr^{6+} are ion exchange, adsorption/biosorption, coagulation-flocculation, chemical precipitation, electrochemical method, biological reduction, and membrane filtration [4]. Although these techniques are highly promising, long-term applications are often hindered due to high operational/maintenance costs, additional energy requirement, and the formation of large secondary toxic sludge.

In the past decade, microbial fuel cells (MFCs) have received enormous attention as a promising technology for wastewater treatment coupled with electricity generation [5–7]. MFCs are devices that use exoelectrogenic bacteria to oxidize the organic matter in the anode chamber, thereby producing protons and electrons. The

* Correspondence: praveenag@iitpkd.ac.in

¹Department of Civil Engineering, Indian Institute of Technology Palakkad, Palakkad 678557, India

Full list of author information is available at the end of the article



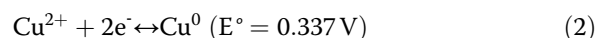
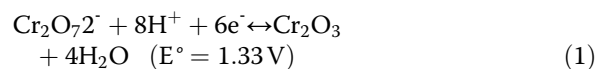
© The Author(s). 2020 **Open Access** This article is licensed under a Creative Commons Attribution 4.0 International License, which permits use, sharing, adaptation, distribution and reproduction in any medium or format, as long as you give appropriate credit to the original author(s) and the source, provide a link to the Creative Commons licence, and indicate if changes were made. The images or other third party material in this article are included in the article's Creative Commons licence, unless indicated otherwise in a credit line to the material. If material is not included in the article's Creative Commons licence and your intended use is not permitted by statutory regulation or exceeds the permitted use, you will need to obtain permission directly from the copyright holder. To view a copy of this licence, visit <http://creativecommons.org/licenses/by/4.0/>.

protons drift internally through a proton exchange membrane (PEM), while the electrons migrate externally to the cathode chamber, where they are reduced to form water by an appropriate catholyte [8, 9]. The anode chamber of the MFC is highly versatile to treat simple organic compounds like acetate [10] and glucose [11] to complex wastewater such as brewery [12], distillery [13], and starch [14]. Besides, the cathode chamber of the MFC is successfully employed for treating metal-laden wastewater containing single metal ions such as cobalt [15], copper [16], silver [17], chromium [3, 18], and selenite [19]. Although MFCs offer promising solutions for the removal of Cr^{6+} [3, 18], the slow reaction kinetics and long operating time due to high cathodic overpotential hinder it from large-scale applications [20, 21]. Recently, Krishnani et al. [22] utilized various conductive polymers such as polyaniline, polypyrrole, polyaniline nanowires and palladium-decorated polyaniline for Cr^{6+} reduction due to their electrical properties (like that of a semiconductor) and mechanical strength. Pang et al. [20] have reported an MFC employed with graphite felt coated conductive polypyrrole that reduces the cathodic overpotential and improves the electron shuttling at the cathode-catholyte interface for Cr^{6+} reduction. Nevertheless, their long-term applications are still limited due to complicated synthesis methods, poor dispersibility, weak stability, and low conductivity [23].

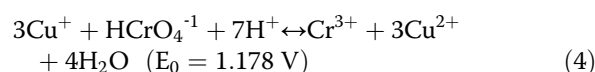
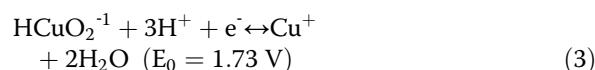
Recently, environmentally benign and cost-effective dissolved cathodic electron-shuttle mediators (dcESMs) have drawn wide attention as they mediate and expedite the reduction of Cr^{6+} in MFC. The dcESM can encourage electron transfer between the microbes or from cathode to the microbes, and/or from microbes to the electron-accepting compounds [24]. They exhibit reversible redox reactions and thereby improve the kinetics of Cr^{6+} reduction by diminishing the electrical repulsion between the negatively charged cathode and the electron acceptors ($\text{Cr}_2\text{O}_7^{2-}$ or CrO_4^{2-}) [21, 25]. Also, due to their high solubility, they can quickly equilibrate the charges with cathode and electron-accepting substances. Liu et al. [26] reported improved reduction of Cr^{6+} using H_2O_2 as a dcESM. However, its long-term operation was hindered due to poor oxygen reduction kinetics. Wang et al. [21] noticed Fe^{3+} as a dcESM, decreases diffusion resistance and cathodic overpotential, and hence enhances the Cr^{6+} reduction. Although Fe^{3+} improves the Cr^{6+} reduction, the power production was decreased by 36% due to the loss of Fe^{3+} via reduction.

As an alternative, copper (Cu^{2+}) can be used as a dcESM due to its excellent catalytic behavior. Cu^{2+} improves the biocathode performance in MFC by promoting the electron transfer between cathode and microbes [27–29]. Recently, Li and Zhou [25] have explored Cu^{2+} as a sole dcESM for Cr^{6+} reduction in the abiotic

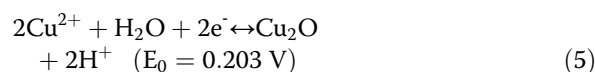
cathode of the MFC. When Cu^{2+} is employed as a dcESM for Cr^{6+} reduction, the high reduction potentials of Cr^{6+} and Cu^{2+} (at 25 °C; Eqs. (1) and (2), respectively) lead them electrochemically reduce to chromium oxide (Cr_2O_3) and Cu^0 , respectively under closed-circuit conditions of the MFC [2, 25, 30].



However, the dcESM behavior of Cu^{2+} is precisely influenced by cathode potential (E_h) and pH of the catholyte [16]. The E_h and pH of Cu^{2+} mediated Cr^{6+} reduction is calculated (calculations are shown in the [Supplemental Materials](#)) and is shown in Fig. 1a. When pH drops below a critical value ($\text{pH} \leq 3.2$; Fig. 1a), Cu^{2+} behaves as a dcESM by undergoing a redox process which expedites the reduction of Cr^{6+} as shown in Eqs. (3) and (4) (at 25 °C). For instance, Cu^{2+} that are reduced to Cu^{1+} acts as the electron donor for the reduction of Cr^{6+} to Cr^{3+} , while at the same time, the Cu^{1+} is oxidized back to Cu^{2+} (Eqs. (3) and (4)). This is because, when pH drops below a critical value, the oxidation state of Cu is +2 (Fig. 1a); hence, it undergoes the redox process and exhibits dcESM phenomenon. While the valence state of Cr is +6 and it thermodynamically favors the reduction of Cr^{6+} to Cr^{3+} in the presence of an ideal electron donor, Cu^{2+} .



On the other hand, at pH above a critical value ($\text{pH} \geq 3.2$), Cu^{2+} undergo reduction to stable cuprous oxide (Cu_2O) (Eq. (5) and Fig. 1a), hindering the dcESM performance of Cu^{2+} on Cr^{6+} reduction.



Although the mechanism of Cu^{2+} in mediating Cr^{6+} reduction has been demonstrated, the dcESM behavior of Cu^{2+} , particularly in acidic conditions, has not yet been reported in any literature. Hence, the present study intends to: (i) demonstrate the dcESM behavior of Cu^{2+} on Cr^{6+} reduction at pH 2 and 4 (the two pH conditions were selected based on the above theoretical evidence) using carbon cloth (CC) as the electrode in MFC and elucidate the mechanism by cyclic voltammetry (CV) analysis; (ii) determine the effect of Cu^{2+} concentration

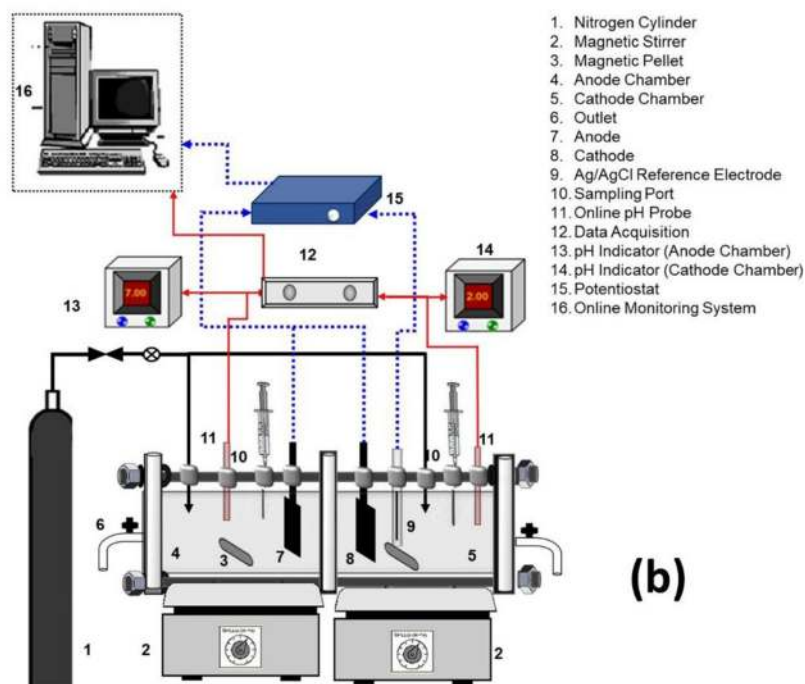
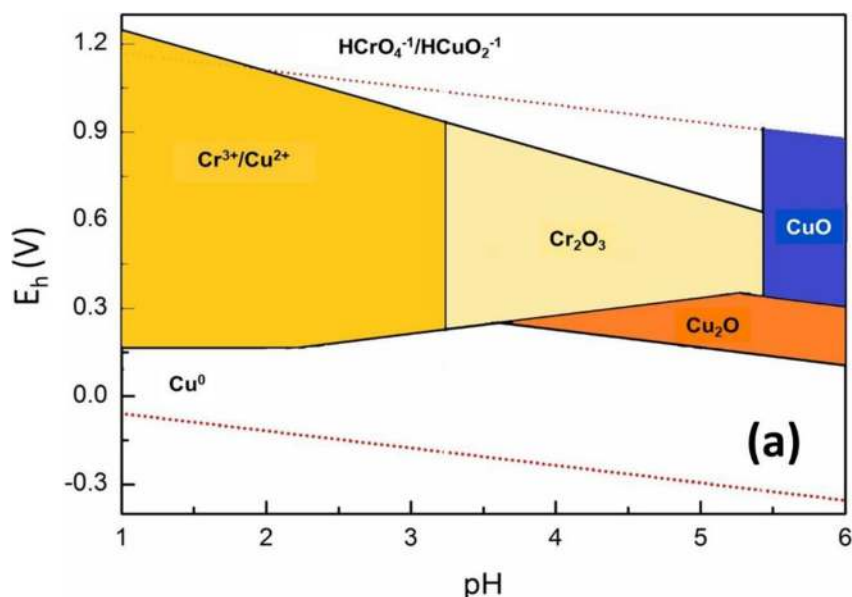


Fig. 1 **a** The equilibrium E_h -pH diagram of Cr-Cu-H₂O system; **b** The experimental set-up of MFC

for Cr⁶⁺ reduction and electricity production in the MFC; and (iii) compare the performance of Cu²⁺ as dcESM on CC with carbon felt (CF) and platinum (Pt) cathodes in the MFC for Cr⁶⁺ reduction and electricity generation.

Materials and methods

MFC construction

The experimental setup of an MFC is shown in Fig. 1b. A two-chambered reactor (each chamber

having dimensions 10.5 × 10 × 12 cm; 500 mL capacity; 300 mL working volume) was made with a plexiglass acrylic tube. The chambers were arranged directly adjacent to each other by a PEM (Nafion 117; Sigma-Aldrich; projected surface area of 50.24 cm²), and a square-ring with rubber gaskets were held in between the PEM to maintain air-tight condition. PEM was subsequently pretreated with 30% H₂O₂, deionized water, 0.5 M H₂SO₄, and deionized water again, for 1 h each [31].

The anode was made up of a low molecular heterocyclic aminopyrazine (Apy)-reduced graphene oxide (r-GO) hybrid coated CC (r-GO-Apy-CC; 25 cm²). The anode material was selected based on one of our previous studies [23], where the r-GO-Apy-CC electrode was found to exhibit excellent bioelectrocatalytic activity for both bacterial adhesion and current generation. Electrodes such as CC (25 cm²; Synergic India Pvt. Ltd. India), CF (25 cm²; Synergic India Pvt. Ltd. India) and Pt (25 cm²; Kevin Scientific, Chennai) were used as cathodes, and are connected externally to the anode by a copper wire. The electrodes were previously soaked in deionized water for 24 h, subsequently dried in the oven at 100 °C for 15 min and were placed at 5 cm apart on either side of the PEM. The anode and cathode chambers were continuously purged with nitrogen to maintain anaerobic conditions. The anodic and cathodic pH was continuously monitored by employing an online pH sensor provided with a multi-channelled data acquisition system (Aqua controller Model 980 AP, Adsensor; India). Fluctuations in the pH of the two chambers were monitored by using online indicators (Fig. 1b).

Inoculation

The anode chamber of the MFC was inoculated with anaerobic sludge collected from anaerobic digester of the sewage treatment plant, Nesapakkam, Chennai, India. The sludge was washed with 0.85% NaCl (w/v) solution and subjected to heat shock pretreatment (100 °C, 2 h) to suppress the activity of methanogens [32]. Sodium acetate (pH value 7.0) was used as the carbon source in the anode chamber of the MFC. For inoculation, 50 mL of dewatered anaerobic sludge was added to 250 mL of synthetic wastewater containing macronutrients as NH₄Cl, 125 mg L⁻¹; NaHCO₃, 125 mg L⁻¹; MgSO₄·7H₂O, 51 mg L⁻¹; CaCl₂·2H₂O, 300 mg L⁻¹; FeSO₄·7H₂O, 6.25 mg L⁻¹ and 1.25 mL L⁻¹ of trace metal solution as reported in Lovley and Phillips [33]. Nitrogen gas was purged continuously to maintain anaerobic conditions in the anode and cathode chambers. Synthetic electroplating wastewater was used as a catholyte and was prepared by mixing an appropriate quantity of potassium dichromate (K₂Cr₂O₇; 99%; Sigma-Aldrich) and copper sulfate (CuSO₄; 99%; Sigma-Aldrich) with deionized water. The initial concentrations of Cu²⁺ and Cr⁶⁺ were maintained at 100 mg L⁻¹. To study the effect of Cu²⁺ concentration on Cr⁶⁺ reduction, the initial concentration of Cr⁶⁺ was maintained at 100 mg L⁻¹, and the different concentrations of Cu²⁺ of 50, 100, 300, 500 mg L⁻¹ were added. The conductivity of the catholyte was improved by adding NaCl (11.7 g L⁻¹). The pH of the influent solution was adjusted with H₂SO₄ (0.1 M) and NaOH (0.1 M). All the experiments were carried out at ambient temperature.

Measurements and analyses

Hexavalent chromium was analyzed by UV-Vis spectrophotometer (UV-1800 PC, Shimadzu) at 540 nm. Total copper was measured using Atomic Absorption Spectrophotometry (AAAnalyst 700, Perkin Elmer) after sampling at regular intervals. The removal efficiency was calculated using Eq. (6).

$$\text{Removal efficiency (\%)} = \frac{(A - B)}{A} \times 100 \quad (6)$$

where A and B are the initial and observed concentrations in mg L⁻¹.

A precise 4-channel potentiostat (VSP 300 Biologic; India) was employed to investigate the electrochemical characteristics of the system. Current (I) was calculated according to Ohm's law, $I = V/R$, where R is the external resistance. Power (P) is the product of voltage V and I ($P = IV$). Power and current densities were calculated by dividing the respective terms by the cathode surface area (m²). The polarization study was performed by employing the I-V characterization technique using a three-electrode system, where the working electrode was a cathode, the counter electrode was an anode, and reference electrode was saturated Ag/AgCl (+0.197 V vs. SHE), that was placed close to the cathode.

The electrochemical activity of the electrode was examined by CV analysis in a separate single-cell system. The experiment was performed in a high purity quartz glass beaker (500 mL) with an airtight polytetrafluoroethylene cap, mounted over silicon encapsulated polytetrafluoroethylene ring. The cell system consists of a counter electrode of standard Pt, reference electrode of Ag/AgCl, and the working electrode of CC. CV analysis was conducted in the cell system deployed with Cu²⁺ mediated Cr⁶⁺ solution (1:1), and the performance was compared with a controlled solution of Cr⁶⁺ and Cu²⁺ solution. During CV analysis, the working electrode potential in controlled Cu²⁺ and Cu²⁺ mediated Cr⁶⁺ solutions were linearly scanned from +1 V to -1 V at a scan rate of 10 mV s⁻¹. In controlled Cr⁶⁺ solution, the potential was linearly scanned from +0.5 to +1.5 V for pH 2, and +0.5 to 1.0 V for pH 4 at a scan rate of 10 mV s⁻¹. High-resolution scanning electron microscopy (FEI Quanta 200 FEG) equipped with energy-dispersive x-ray spectroscopy was employed to confirm Cr³⁺ and Cu₂O monolayer formation on cathode surfaces for a specific period.

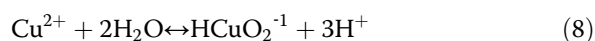
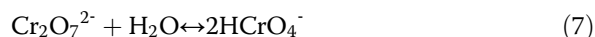
Results and discussion

The dcESM behavior of Cu²⁺ for Cr⁶⁺ reduction

The dcESM behavior of Cu²⁺ on Cr⁶⁺ reduction (initial concentrations of 100 mg L⁻¹; 1:1 ratio) was characterized on CC cathode in MFC at pH 2 and 4. The temporal behavior of Cu²⁺ and Cr⁶⁺, and corresponding

variations in pH were monitored at pH 2 and 4. The experimental result at pH 2 displays a large reduction in Cr^{6+} to Cr^{3+} with an efficiency of 99.9% at 84 h of operating time (Fig. 2a). In contrast, the reduction of Cu^{2+} was not significant at pH 2. A slight decrease (25%) in the Cu^{2+} concentration was noticed within the initial few hours, probably, due to the reduction of Cu^{2+} to Cu^{1+} (Eq. (3)). However, at pH 4, a considerable reduction of Cu^{2+} along with Cr^{6+} was observed.

The results were interpreted that the reduction of Cr^{6+} in the presence of Cu^{2+} involves heterogeneous reactions. At pH 2, Cr^{6+} and Cu^{2+} are highly protonated by surrounding the H^+ ions and predominantly exist in the form of HCrO_4^{-1} and HCuO_2^{-1} , respectively as shown in the reactions Eqs. (7) and (8). During the initial 10 h, a decrease in the pH was noticed from the initial pH (pH 2) due to the hydrolysis of Cu^{2+} which involves an increase in the H^+ ions in the solution as shown in Eq. (8).

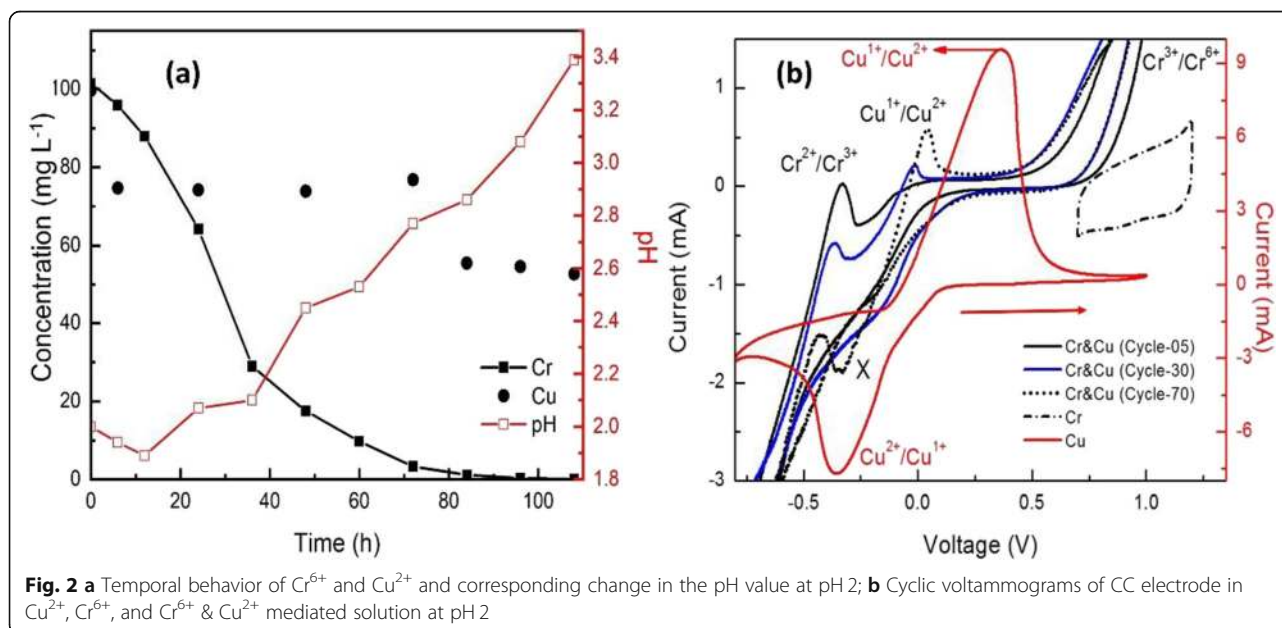


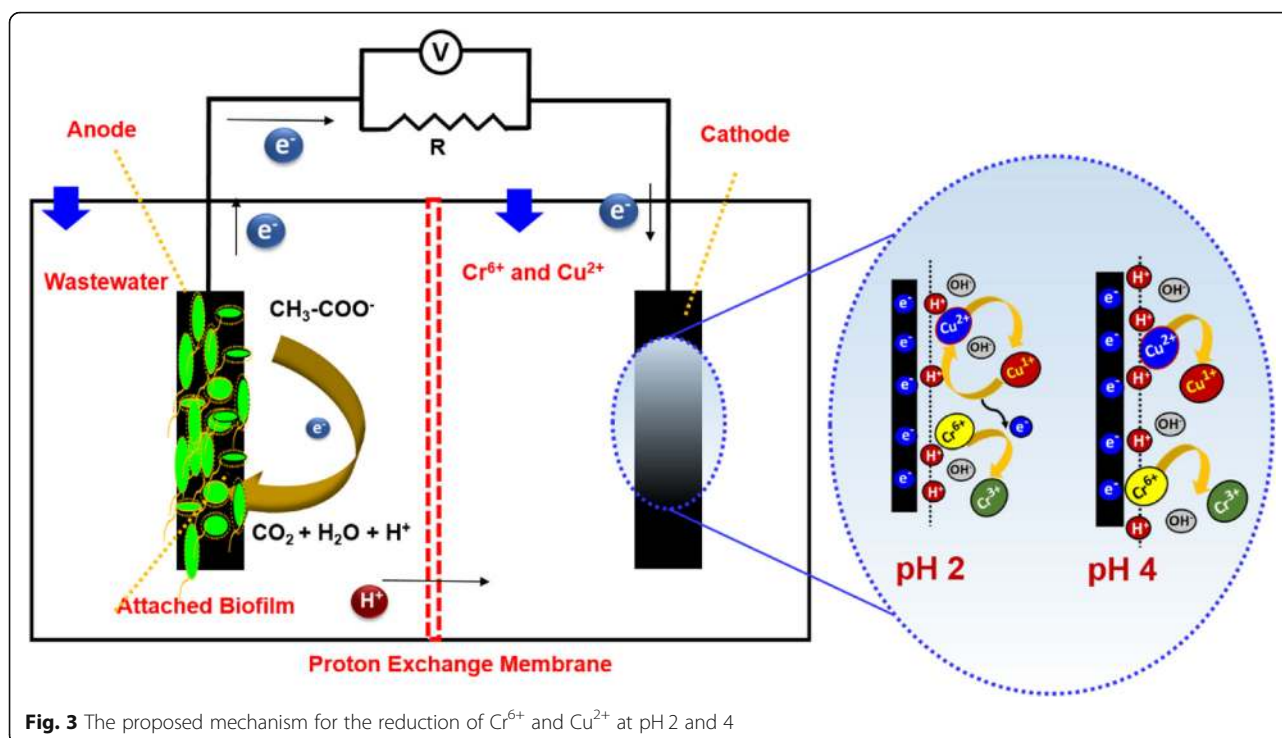
Besides, a slight reduction in the Cu^{2+} (25%) was observed at this stage, probably due to the cathodic reduction of HCuO_2^{-1} to Cu^+ in the presence of H^+ ions as explained in Eq. (3) [34]. However, a steady-state reduction in Cr^{6+} concentration was observed throughout the experiment. This could be correlated with Eqs. (3) and (4) and explained as: the Cu^{2+} that is reduced to Cu^{1+} acts as an electron donor for the reduction of Cr^{6+} to Cr^{3+} , while at the same time, the Cu^{1+} is oxidized back to Cu^{2+} . Correspondingly, the pH of catholyte was increased owing to the consumption of H^+ ions as

indicated in Eqs. (3) and (4). The color of the wastewater was changed from orange-yellow to greenish-yellow after 48 h, indicating, the complete reduction of Cr^{6+} to Cr^{3+} .

A separate CV analysis was conducted to confirm the dcESM behavior of Cu^{2+} on Cr^{6+} reduction at pH 2 using a single cell system with CC as a working electrode (Fig. 2b). At pH 2, CV analysis of controlled Cu^{2+} solution exhibits well-defined reduction and oxidation peaks at -0.36 and $+0.36$ V, respectively, which could be attributed to the dcESM behavior of Cu^{2+} on CC electrode (Fig. 2b) [35]. In a mixture of Cu^{2+} and Cr^{6+} solution, CV analysis was repeated for 70 cycles at a scan rate of 10 mV s^{-1} . During the forward scan, a large cathodic current was drawn after 0.23 V was due to the combined reduction of Cu^{2+} and Cr^{6+} , and on the reverse scan, the peak observed at -0.34 V was correlated with the oxidation of Cr^{2+} to Cr^{3+} (Cycle 5; Fig. 2b) [36]. The additional peak observed at -0.01 V (Cycle 30; Fig. 2b) can be attributed to the oxidation of Cu^{1+} to Cu^{2+} . While continuing the scan up to 70 cycles, the peak at -0.34 V was observed to be diminished due to the stable and insoluble Cr^{3+} formation. Concurrently, the peak observed at -0.01 V was found to increase due to the increases in Cu^{1+} concentration. The CV study confirms the dcESM behavior of Cu^{2+} on Cr^{6+} reduction at pH 2 and complements with the reported experimental results.

The proposed mechanism for the reduction of Cr^{6+} and Cu^{2+} at pH 2 and 4 are shown in Fig. 3. At pH 4, simultaneous reduction of Cu^{2+} and Cr^{6+} was observed with removal efficiencies of 71 and 56%, respectively (Fig. 4a). At this pH condition, dcESM behavior of Cu^{2+} was not observed; instead, simultaneous reduction of Cr^{6+} and Cu^{2+} was noticed. This could be due to the





stable form of Cu_2O which hinders the dcESM behavior of Cu^{2+} for Cr^{6+} reduction. However, simultaneous reductions of Cu^{2+} and Cr^{6+} were occurred owing to the high cathodic potential as presented in Eqs. (1) and (5). The pH was observed to increase from 4 to 5.54 and the color of the effluent was changed from orange-yellow to pale yellow. In CV analysis, the peak observed at -0.34 and -0.01 V at pH 2 conditions were absent at pH 4 and can be attributed to the irreversibility of the Cu^{2+} and Cr^{6+} as stable Cu_2O and Cr_2O_3 , respectively (Fig. 4b).

Effect of Cu^{2+} concentration on Cr^{6+} reduction and electricity production

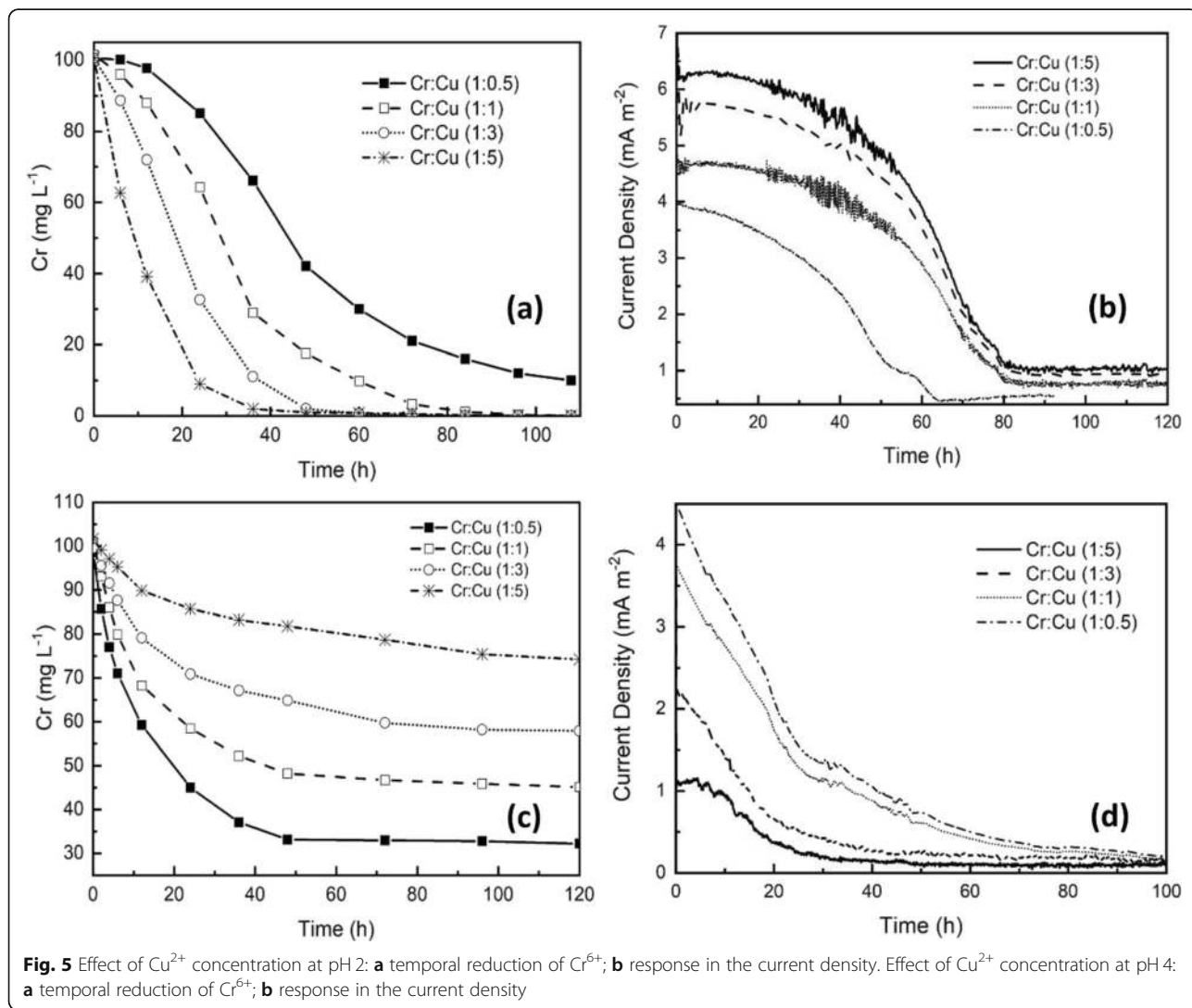
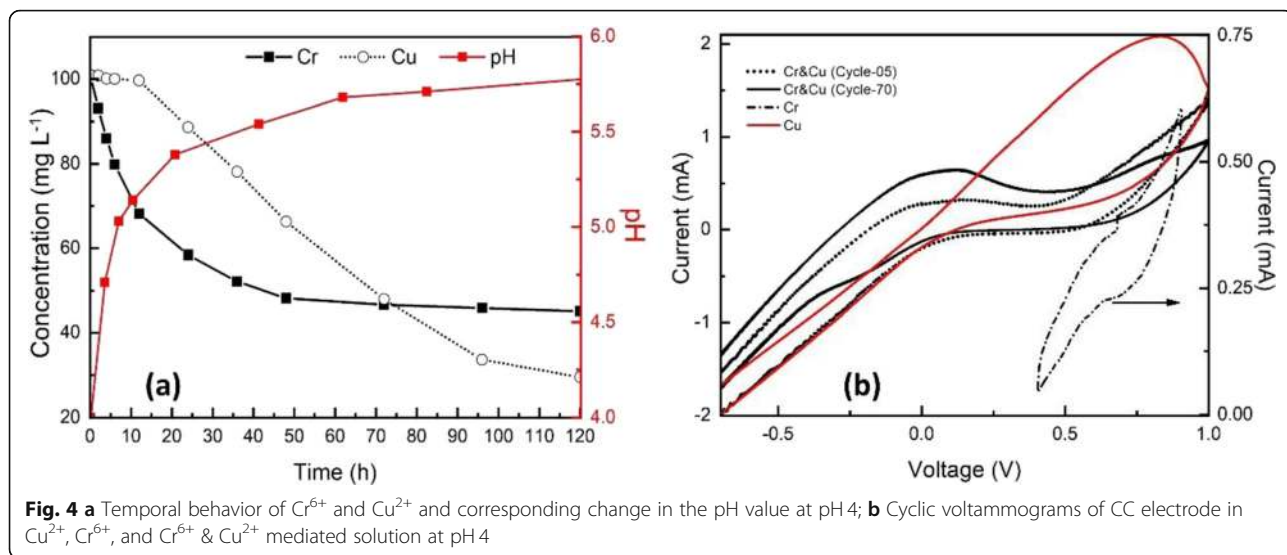
Studies were performed by varying the Cu^{2+} concentration at pH 2 and 4 to understand the effect of Cu^{2+} and its dcESM behavior on Cr^{6+} reduction and bioelectricity generation. The results elucidate that, at pH 2, the presence of Cu^{2+} is highly favorable for the reduction of Cr^{6+} . Increasing the Cu^{2+} concentration from 50 to 500 mg L^{-1} reduces reaction time from 108 to 48 h for the complete reduction of Cr^{6+} (Fig. 5a). Similarly, the current production was improved from 3.94 to 6.24 mA m^{-2} by increasing the Cu^{2+} concentration from 50 to 500 mg L^{-1} (Fig. 5b). However, at pH 4, the presence of Cu^{2+} decreases the reduction of Cr^{6+} . By increasing the Cu^{2+} concentration from 50 to 500 mg L^{-1} , the reduction efficiency of Cr^{6+} was observed to decrease from 63 to 18% (Fig. 5c). Correspondingly, the response in the current density was decreased from 4.4 mA m^{-2} (616 mV) to 1.1 mA m^{-2} (155 mV), respectively (Fig. 5d).

At pH 2, increasing the Cu^{2+} concentration improves the reduction of Cr^{6+} and electricity generation from MFC. This could be due to the dcESM behaviour of Cu^{2+} improves the kinetics of Cr^{6+} reduction by diminishing the electrical repulsion between the negatively charged cathode and the $\text{Cr}_2\text{O}_7^{2-}$ anions in the catholyte [21, 25]. As the rate of electron transfer improves, the cathodic over potential decreases resulting in an improvement in the generation of electricity. On the other hand, at pH 4, increasing the concentration of Cu^{2+} decreases the reduction kinetics of Cr^{6+} as well as the responses in the current density. At pH 4, Cu^{2+} was electrochemically reduced to Cu_2O (Eq. (5) and Fig. 1a) and deposited over the electrode surface (Fig. 7b). The deposition of Cu_2O increases with increase in the Cu^{2+} concentration. This results in higher cathodic overpotential at the cathode-catholyte interface that hinders the kinetics of Cr^{6+} reduction and current production at pH 4. In both the pH conditions, the temporal response of the current density was found to be decreased as the experiment progresses. The trend can be correlated with the decrease in the catholyte concentration due to the reduction of Cr^{6+} and can be theoretically explained by the Nernst equation as in Eqs. (9) and (10).

$$E_{\text{cathode}} - E_0 = - \frac{2.303 RT}{nF} \log \frac{[\text{Cr}^{3+}]}{[\text{Cr}^{6+}]} \quad (9)$$

$$\eta_c = - \frac{2.303 RT}{nF} \log \frac{[\text{Cr}^{3+}]}{[\text{Cr}^{6+}]} \quad (10)$$

According to the Eq. (10), overpotential (η_c) becomes more negative as the concentration of Cr^{3+} increases,



causing a decrease in the cell potential [37, 38]. Eventually, the response in the current density decreases as the experiment progresses. When the rate of reduction of Cr^{6+} reaches an asymptotic state, the response of the current density exhibits an analogous behavior to the concentration of Cr^{6+} .

The dcESM behavior of Cu^{2+} on CF and Pt electrodes

The dcESM behavior of Cu^{2+} on Cr^{6+} reduction (initial concentrations of 100 mg L^{-1} ; 1:1 ratio) was characterized on Pt and CF in MFC at pH 2 (Fig. 6a) and pH 4 (Fig. 6b), and the results were compared with CC electrode. It was observed that, at pH 2, the reduction of Cr^{6+} to Cr^{3+} in 60 h is 99.8% for CF cathode, 48% for Pt cathode, and 90% for CC cathode. As expected, not much reduction of Cu^{2+} occurred in all the electrodes at pH 2 (Fig. 6a). The color of the wastewater was changed from orange-yellow to greenish-yellow, and subsequently, a stable blue color solution when CC and CF were employed as the cathode material. However, in the case of Pt as a cathode, the color of the wastewater was changed moderately from orange-yellow to pale yellow. At pH 4, the simultaneous reduction of Cr^{6+} and Cu^{2+} was observed for Pt and CF electrodes. The reduction of Cr^{6+} at pH 4 in 120 h is 68% for CF cathode, 29% for Pt cathode, and 56% for CC cathode (Fig. 6b). Similarly, Cu^{2+} reduction in 120 h is 75% for CF cathode, 50% for Pt cathode, and 71% for CC cathode. The results indicate that the dcESM behavior of Cu^{2+} on Cr^{6+} reduction is exhibited not only on CC but also in CF and Pt cathodes in MFC.

The surface morphological characteristics of the Cr^{3+} and Cu_2O on the surface of Pt, CC, and CF were analyzed by performing the SEM analysis (Fig. 7a, b, and c, respectively), and the image clearly shows the nucleation of Cr^{3+} or Cr_2O_3 and/or Cu_2O on the cathode surface. Furthermore, polarization studies were performed with

CC, CF and Pt to understand the efficiency of electrode material for power production (Fig. 7d). The maximum power densities of 1659 mW m^{-2} (4.9 mA m^{-2}), 1509 mW m^{-2} (5.5 mA m^{-2}), and 1284 mW m^{-2} (5.1 mA m^{-2}) were achieved when CF, CC, and Pt were employed as cathode materials. The study confirms that carbon-based electrode materials are ideal for bioelectricity generation from MFC.

Practical implication to scale up MFC technology

In summary, MFCs apply a simple redox principle in which the sole influencing factor for the entire electrochemical reductions is the degradation of organic matter (The details are provided in [Supplementary Materials](#)) by exoelectrogenic microorganisms at the anode chamber. At the cathode, Cr^{6+} electrochemically reduces to Cr^{3+} by accepting the electrons from the anode chamber. The use of dissolved electron-shuttle mediators reduces the activation energy at the cathode-electrolyte interface and improves the cathode performance for Cr^{6+} reduction and bioelectricity generation. In fact, Cu^{2+} is a potential contaminant, and extreme consumption of copper leads to severe toxicological concerns, such as nausea, contractions, convulsions, or even death [16, 39]. Hence, incorporating Cu^{2+} as a dissolved mediator in MFC is a sustainable approach because Cu^{2+} not only enhances the reduction of Cr^{6+} but also reduces to its most stable, Cu_2O form, simultaneously. The findings demonstrated in the present study are highly significant to the electroplating industry where a combination of Cr^{6+} and Cu^{2+} are discharged at high acidic conditions from washing, rinsing, batch dumps, and processing and/or operational units. Presently, chemical coagulation/precipitation is the most widely adopted treatment technique for electroplating wastewater. However, this technique involves high operational costs due to the

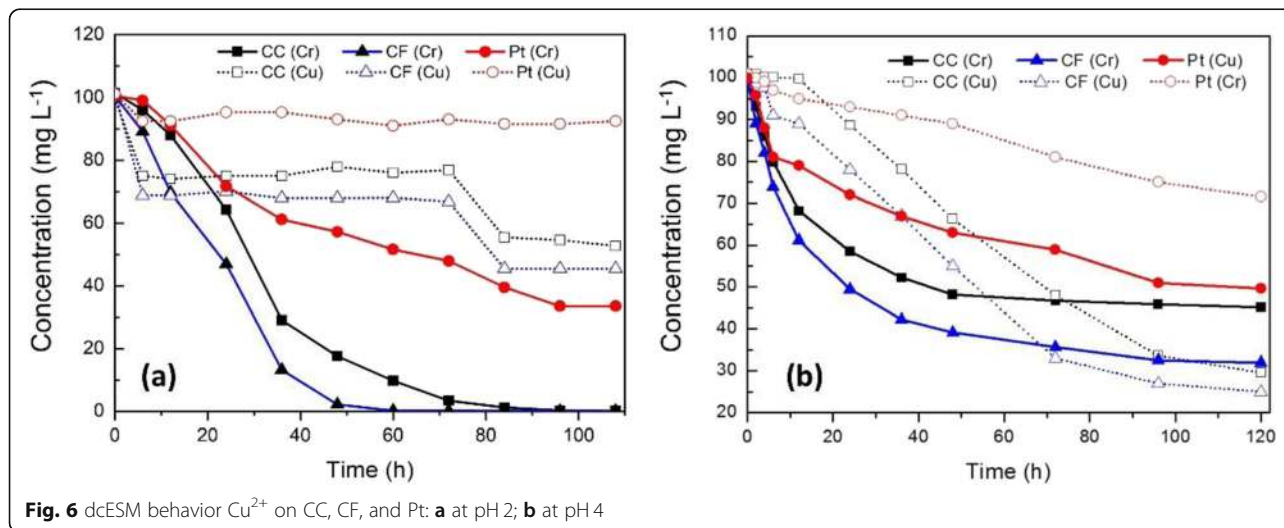


Fig. 6 dcESM behavior Cu^{2+} on CC, CF, and Pt: **a** at pH 2; **b** at pH 4

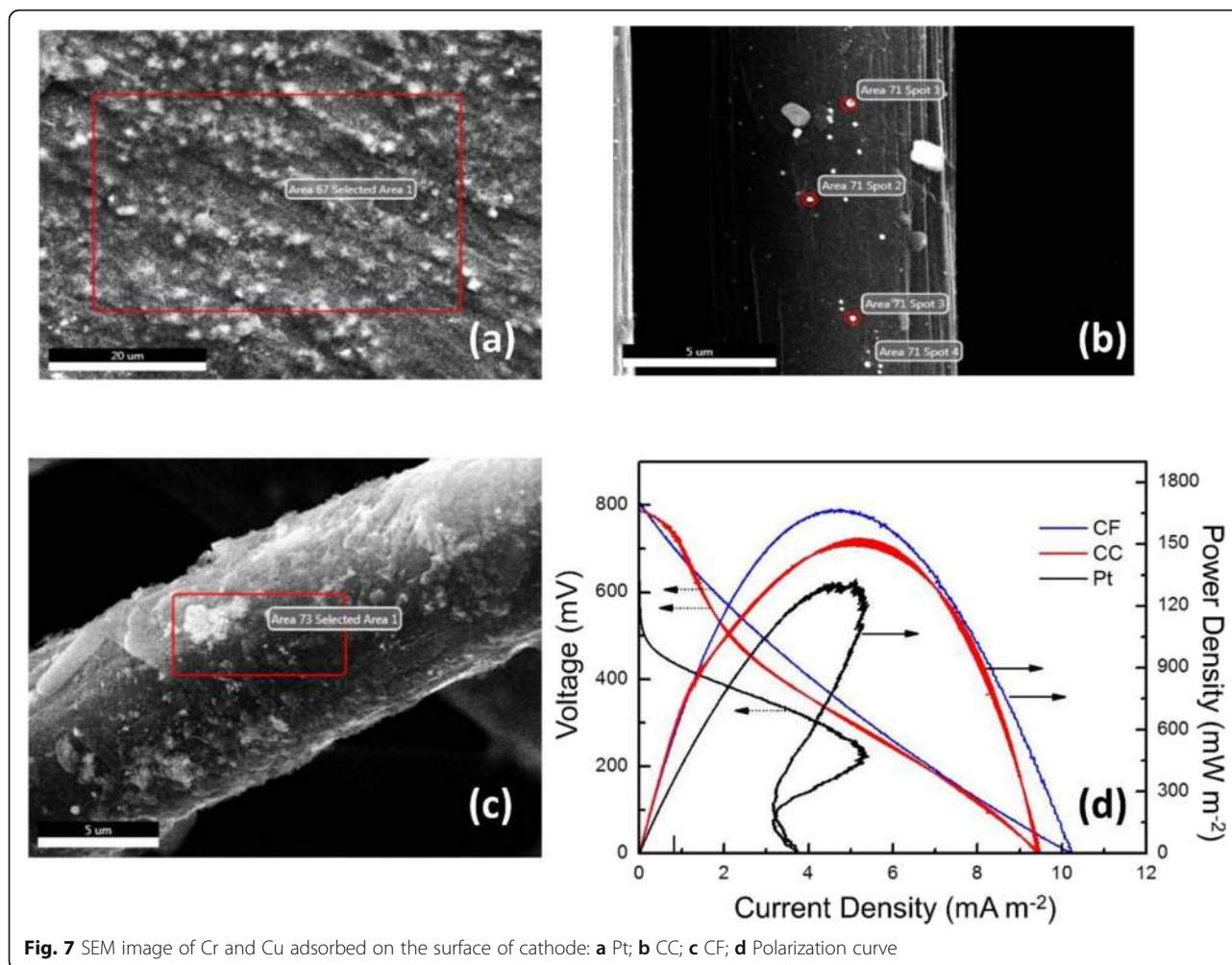


Fig. 7 SEM image of Cr and Cu adsorbed on the surface of cathode: **a** Pt; **b** CC; **c** CF; **d** Polarization curve

consumption of large amounts of chemicals and the generation of a huge quantity of sludge. Instead, the use of Cu^{2+} as a dcESM for Cr^{6+} reduction is a cost-effective method as it does not require any addition of chemicals, and both often co-exist in the effluents discharged from electroplating or mining industries. However, further studies are required to evaluate the long-term operation conditions and process economy of MFC over influent. Also, pilot/full-scale studies are needed for the practical implementation of this technology in industries.

Conclusions

In the present work, dcESM phenomenon of Cu^{2+} on Cr^{6+} reduction in MFC is reported using CC, CF, and Pt electrodes. The dcESM behavior of Cu^{2+} for Cr^{6+} reduction is highly influenced by E_h and pH of the catholyte in MFC. In acidic conditions, when the pH is below a critical point of 3.2, Cu^{2+} improves the reduction of Cr^{6+} to 99.9% at 84 h of operating time. On the other hand, above the critical pH point, simultaneous reduction of Cu^{2+} and Cr^{6+} was observed with removal efficiencies of

71 and 56%, respectively. Hence, the Cu^{2+} and its role as dcESM in MFC is highly advantageous as it not only enhances the Cr^{6+} reduction but also undergoes electrochemical reduction into non-toxic Cu_2O . Since Cu^{2+} on Cr^{6+} often co-exist in the wastewater from electroplating or mining industries, and due to their synergy, the study provides an entirely new concept of 'using a pollutant to treat another one' with simultaneous generation of energy.

Supplementary information

Supplementary information accompanies this paper at <https://doi.org/10.1186/s42834-020-00059-3>.

Additional file 1. .

Acknowledgements

The authors gratefully acknowledge the financial support of DST, India [No. SR/WOS-A/ET-1017/2014] in carrying out this research work.

Authors' contributions

Praveena Gangadharan planned and conducted the experiments. Indumathi M Nambi supervised the project. The author(s) read and approved the final manuscript.

Funding

This work was supported by DST, India [No. SR/WOS-A/ET-1017/2014].

Availability of data and materials

The data used to support the findings of this study are available from the corresponding author upon request.

Competing interests

The authors declare that they have no competing interests.

Author details

¹Department of Civil Engineering, Indian Institute of Technology Palakkad, Palakkad 678557, India. ²Department of Civil Engineering, Indian Institute of Technology Madras, Chennai 600036, India.

Received: 16 April 2020 Accepted: 30 July 2020

Published online: 10 September 2020

References

- Sivapirakasam SP, Mohan S, Kumar MCS, Paul AT, Surianarayanan M. Control of exposure to hexavalent chromium concentration in shielded metal arc welding fumes by nano-coating of electrodes. *Int J Occup Env Heal*. 2017; 23:128–42.
- Nancharaiyah YV, Mohan SV, Lens PNL. Biological and bioelectrochemical recovery of critical and scarce metals. *Trends Biotechnol*. 2016;34:137–55.
- Gangadharan P, Nambi IM. Hexavalent chromium reduction and energy recovery by using dual-chambered microbial fuel cell. *Water Sci Technol*. 2015;71:353–8.
- Kurniawan TA, Chan GYS, Lo WH, Babel S. Physico-chemical treatment techniques for wastewater laden with heavy metals. *Chem Eng J*. 2006;118:83–98.
- Rabaey K, Verstraete W. Microbial fuel cells: novel biotechnology for energy generation. *Trends Biotechnol*. 2005;23:291–8.
- Logan BE, Hamelers B, Rozendal RA, Schrorder U, Keller J, Freguia S, et al. Microbial fuel cells: methodology and technology. *Environ Sci Technol*. 2006;40:5181–92.
- Santoro C, Arbizzani C, Erable B, Ieropoulos I. Microbial fuel cells: from fundamentals to applications. A review. *J Power Sources*. 2017;356:225–44.
- Zhao F, Harnisch F, Schrorder U, Scholz F, Bogdanoff P, Herrmann I. Challenges and constraints of using oxygen cathodes in microbial fuel cells. *Environ Sci Technol*. 2006;40:5193–9.
- Liu H, Ramnarayanan R, Logan BE. Production of electricity during wastewater treatment using a single chamber microbial fuel cell. *Environ Sci Technol*. 2004;38:2281–5.
- Liu H, Cheng SA, Logan BE. Production of electricity from acetate or butyrate using a single-chamber microbial fuel cell. *Environ Sci Technol*. 2005;39:658–62.
- Chae KJ, Choi MJ, Lee JW, Kim KY, Kim IS. Effect of different substrates on the performance, bacterial diversity, and bacterial viability in microbial fuel cells. *Bioresour Technol*. 2009;100:3518–25.
- Zhuang L, Yuan Y, Wang YQ, Zhou SG. Long-term evaluation of a 10-liter serpentine-type microbial fuel cell stack treating brewery wastewater. *Bioresour Technol*. 2012;123:406–12.
- Ha PT, Lee TK, Rittmann BE, Park J, Chang IS. Treatment of alcohol distillery wastewater using a bacteroidetes-dominant thermophilic microbial fuel cell. *Environ Sci Technol*. 2012;46:3022–30.
- Lu N, Zhou SG, Zhuang L, Zhang JT, Ni JR. Electricity generation from starch processing wastewater using microbial fuel cell technology. *Biochem Eng J*. 2009;43:246–51.
- Huang LP, Li TC, Liu C, Quan X, Chen LJ, Wang AJ, et al. Synergetic interactions improve cobalt leaching from lithium cobalt oxide in microbial fuel cells. *Bioresour Technol*. 2013;128:539–46.
- Tao HC, Liang M, Li W, Zhang LJ, Ni JR, Wu WM. Removal of copper from aqueous solution by electrodeposition in cathode chamber of microbial fuel cell. *J Hazard Mater*. 2011;189:186–92.
- Choi C, Cui Y. Recovery of silver from wastewater coupled with power generation using a microbial fuel cell. *Bioresour Technol*. 2012;107:522–5.
- Gangadharan P, Nambi IM, Senthilnathan J. Liquid crystal polaroid glass electrode from e-waste for synchronized removal/recovery of Cr⁺⁶ from wastewater by microbial fuel cell. *Bioresour Technol*. 2015;195:96–101.
- Catal T, Bermek H, Liu H. Removal of selenite from wastewater using microbial fuel cells. *Biotechnol Lett*. 2009;31:1211–6.
- Pang YM, Xie DH, Wu BG, Lv ZS, Zeng XH, Wei CH, et al. Conductive polymer-mediated Cr (VI) reduction in a dual-chamber microbial fuel cell under neutral conditions. *Synthetic Met*. 2013;183:57–62.
- Wang Q, Huang LP, Pan YZ, Quan X, Puma GL. Impact of Fe (III) as an effective electron-shuttle mediator for enhanced Cr (VI) reduction in microbial fuel cells: reduction of diffusional resistances and cathode overpotentials. *J Hazard Mater*. 2017;321:896–906.
- Krishnani KK, Srinives S, Mohapatra BC, Boddu VM, Hao JM, Meng X, et al. Hexavalent chromium removal mechanism using conducting polymers. *J Hazard Mater*. 2013;252:99–106.
- Gangadharan P, Nambi IM, Senthilnathan J, Pavithra VM. Heterocyclic aminopyrazine-reduced graphene oxide coated carbon cloth electrode as an active bio-electrocatalyst for extracellular electron transfer in microbial fuel cells. *RSC Adv*. 2016;6:68827–34.
- Watanabe K, Manefield M, Lee M, Kouzuma A. Electron shuttles in biotechnology. *Curr Opin Biotech*. 2009;20:633–41.
- Li M, Zhou SQ. Efficacy of Cu (II) as an electron-shuttle mediator for improved bioelectricity generation and Cr (VI) reduction in microbial fuel cells. *Bioresour Technol*. 2019;273:122–9.
- Liu LA, Yuan Y, Li FB, Feng CH. In-situ Cr (VI) reduction with electrogenerated hydrogen peroxide driven by iron-reducing bacteria. *Bioresour Technol*. 2011;102:2468–73.
- Shen JY, Huang LP, Zhou P, Quan X, Li Puma G. Correlation between circuit current, Cu (II) reduction and cellular electron transfer in EAB isolated from Cu (II)-reduced biocathodes of microbial fuel cells. *Bioelectrochemistry*. 2017;114:1–7.
- Tao Y, Xue H, Huang LP, Zhou P, Yang W, Quan X, et al. Fluorescent probe based subcellular distribution of Cu (II) ions in living electrotrophs isolated from Cu (II)-reduced biocathodes of microbial fuel cells. *Bioresour Technol*. 2017;225:316–25.
- Wu YN, Zhao X, Jin M, Li Y, Li S, Kong FY, et al. Copper removal and microbial community analysis in single-chamber microbial fuel cell. *Bioresour Technol*. 2018;253:372–7.
- Nancharaiyah YV, Mohan SV, Lens PNL. Metals removal and recovery in bioelectrochemical systems: a review. *Bioresour Technol*. 2015;195:102–14.
- Li ZJ, Zhang XW, Lei LC. Electricity production during the treatment of real electroplating wastewater containing Cr⁶⁺ using microbial fuel cell. *Process Biochem*. 2008;43:1352–8.
- Mohan SV, Mohanakrishna G, Srikanth S, Sarma PN. Harnessing of bioelectricity in microbial fuel cell (MFC) employing aerated cathode through anaerobic treatment of chemical wastewater using selectively enriched hydrogen producing mixed consortia. *Fuel*. 2008;87:2667–76.
- Lovley DR, Phillips EJP. Novel mode of microbial energy metabolism: organic carbon oxidation coupled to dissimilatory reduction of iron or manganese. *Appl Environ Microb*. 1988;54:1472–80.
- Yamukyan MH, Manukyan KV, Kharatyan SL. Copper oxide reduction by hydrogen under the self-propagation reaction mode. *J Alloy Compd*. 2009; 473:546–9.
- Grujicic D, Pesic B. Electrodeposition of copper: the nucleation mechanisms. *Electrochim Acta*. 2002;47:2901–12.
- De Groot MT, Koper MTM. Redox transitions of chromium, manganese, iron, cobalt and nickel protoporphyrins in aqueous solution. *Phys Chem Chem Phys*. 2008;10:1023–31.
- Plieth W. *Electrochemistry for materials science*. Amsterdam: Elsevier; 2008.
- Perez N. *Electrochemistry and corrosion science*. 2nd ed. Cham: Springer International Publishing; 2016.
- Cheng SA, Wang BS, Wang YH. Increasing efficiencies of microbial fuel cells for collaborative treatment of copper and organic wastewater by designing reactor and selecting operating parameters. *Bioresour Technol*. 2013;147: 332–7.

Publisher's Note

Springer Nature remains neutral with regard to jurisdictional claims in published maps and institutional affiliations.